ACS APPLIED MATERIALS & INTERFACES

Research Article

www.acsami.org

Encapsulation of Hemin in Metal–Organic Frameworks for Catalyzing the Chemiluminescence Reaction of the H_2O_2–Luminol System and Detecting Glucose in the Neutral Condition

Fenqiang Luo,[†] Yaolin Lin,[†] Liyan Zheng,[‡] Xiaomei Lin,[†] and Yuwu Chi*[,†]

[†]MOE Key Laboratory of Analysis Detection Technology for Food Safety, Fujian Provincial Key Laboratory of Analysis and Detection for Food Safety, and College of Chemistry, Fuzhou University, Fuzhou, Fujian 350108, China

[‡]Key Laboratory of Medicinal Chemistry for Natural Resource (Yunnan University), Ministry of Education, School of Chemical Science and Technology, Yunnan University, Kunming, Yunnan 650091, China

Supporting Information

ABSTRACT: Novel metal–organic frameworks (MOFs) based solid catalysts have been synthesized by encapsulating Hemin into the HKUST-1 MOF materials. These have been first applied in the chemiluminescence field with outstanding performance. The functionalized MOFs not only maintain an excellent catalytic activity inheriting from Hemin but also can be cyclically utilized as solid mimic peroxidases in the neutral condition. The synthesized Hemin@HKUST-1 composites have been used to develop practical sensors for H_2O_2 and glucose with wide response ranges and low detection limits. It was envisioned that catalyst-functionalized MOFs for chemiluminescence sensing would have promising applications in green, selective, and sensitive detection of target analytes in the future.

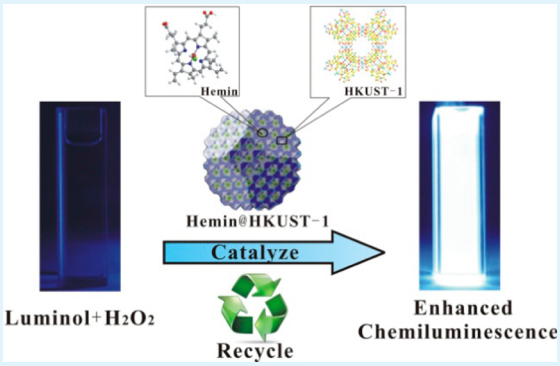

KEYWORDS: *Hemin, HKUST-1, catalysis, chemiluminescence, H_2O_2, glucose*

INTRODUCTION

Metal–organic frameworks (MOFs) are hybrid microporous crystalline materials, self-assembled straightforwardly from metal ions with organic linkers through strong covalent bonds.[1] Specifically, the chemistry of MOFs provides an extensive class of emerging functional materials with high thermal and mechanical stability, tunable metrics, organic functionality, open metal sites in the skeleton, structural diversity, and ultrahigh porosity.[2] Owing to their unusual properties, MOFs have great potential for plenty of applications, such as catalysis,[3,4] separations,[5,6] gas storage,[7−10] ion-exchange,[11,12] sensing,[13] bioimaging, and drug delivery.[14−16]

The use of MOFs for heterogeneous catalysis can be attributed to some advantages of metal–organic framework systems such as the high density of active catalytic centers, great tunability, high level of porosity, crystalline nature enabling elucidation of structural details, and relatively easy immobilization.[17,18] Compared with traditional porous materials such as zeolites and silica, MOFs provide an excellent platform for heterogeneous catalysis.[19] Nowadays, researchers have been attracted by the effect of incorporating active sites in the framework. The incorporated method can bring MOFs some new properties and thus expand their catalytic performance.[20,21] There are several ways of introducing catalytic active sites. One approach is to use the metal or metal cluster connecting points with a free coordinating site as catalytic sites or incorporate an uncoordinated site at one of the metal atoms in the inorganic cornerstone. An alternative approach is to build the active site into the linker, in other words, active catalytic sites can be generated from the functional groups within a MOF scaffold. The attractive and straightforward approach is to entrap active catalysts into MOFs, such as palladium nanoparticles or metalloporphyrins.[22−27]

It is one of the hot trends to incorporate porphyrins or metalloporphyrins into MOFs for a large variety of applications.[28−35] Porphyrins and metalloporphyrins have been extensively studied as chemoselective catalysts.[36] In the homogeneous phase, the dimerization and self-degradation of porphyrins and metalloporphyrins result in their lifetime activity being limited. Therefore, immobilization of porphyrins and metalloporphyrins in solid matrices is expected to enhance stability and protect the active moiety from dimerization.[24]

In 2012, Zhou and co-workers synthesized zirconium–metalloporphyrin PCN-222 to catalyze the oxidation of a variety of substrates.[32] The successful construction of stable 3D structures with large open channels provided an excellent catalytic performance of PCN-222, i.e., several times to over 2 orders of magnitude higher than that of free Hemin in aqueous media. However, the synthesis of the PCN-222 MOFs needed a time-consuming and complicated solvothermal prodedure. Recently, MIL-68, MIL-100, and MIL-53 MOFs have been

Received: February 26, 2015
Accepted: April 30, 2015
Published: April 30, 2015

DOI: 10.1021/acsami.5b01706
ACS Appl. Mater. Interfaces 2015, 7, 11322−11329

Scheme 1. Catalytic Activity and Recyclability of Hemin@HKUST-1 for CL Detection of H_2O_2

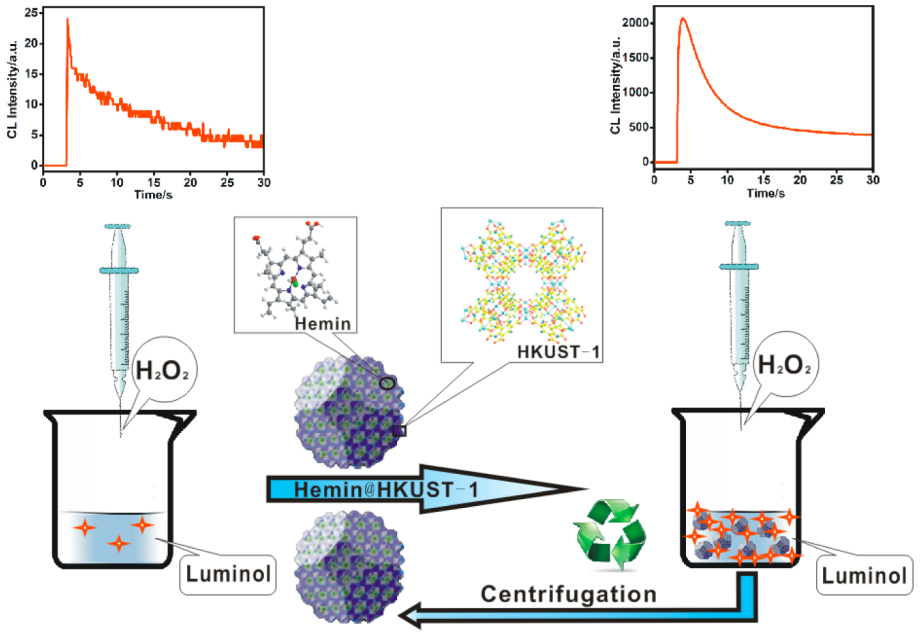

reported as mimic enzyme for colorimetric biosensing of ascorbic acid.[37,38] However, critic experimental conditions such as high temperature and pressure were required to obtain these MOFs. Additionally, the catalytic activities of these MOFs were relatively poor compared with natural enzymes. Therefore, we are interested in searching a kind of MOFs with excellent peroxidase-like activity that can be synthesized quickly and easily.

In 2011, Larsen and co-workers reported a simple method to encapsulate heme into HKUST-1 MOFs and mimick heme enzymes in the solid state.[39] Besides, it is well-known that Hemin can catalyze chemiluminescence (CL) reaction of H_2O_2 and luminol.[40] Inspired by this reported work on MOFs and the previous research on the catalytic property of Hemin,[41,42] we have encapsulated Hemin into HKUST-1 and utilized the obtained Hemin@HKUST-1 for catalyzing CL reaction between H_2O_2 and luminol (Scheme 1). Since its high sensitivity, low background interference, and simple instrumentation, CL detection is applied in many fields. To the best of our knowledge, there is no report on using functionalized MOFs as a platform for CL sensing yet. Therefore, the combination of MOFs with chemiluminescence for analytical chemistry is meaningful. The present work might have following major advantages: (1) Compared with the previously reported MOFs, our Hemin@HKUST-1 can be obtained in a very simple and easy way, e.g. only 7 h-reaction time, 60 °C-reaction temperature, and ambient pressure are required. (2) The synthesized Hemin@HKUST-1 MOF composites not only exhibit good catalytic activity inheriting from molecular Hemin but also can be recycled easily as solid catalysts due to their good stability and easy separation from reaction solutions. (3) For the first time, the Hemin@HKUST-1 MOF composites have been used for developing green, selective, and sensitive CL sensors for the detection of H_2O_2 and glucose.

EXPERIMENTAL SECTION

Chemicals and Materials. 1,3,5-Benzene tricarboxylate (≥98%) and glucose oxidase from *Aspergillus niger* (GOx, 100 U/mg) were bought from Aladdin (Shanghai, China). Hemin (≥98%) was obtained from Alfa Aesar (Shanghai, China); $Cu(NO_3)_2{\cdot}3H_2O$ was received from Fuchen chemical reagent company (Tianjin, China). All other reagents were analytically pure. Doubly distilled water was used throughout the experiments. Here, 0.01 M phosphate buffer solutions (PBS) with different pH were used to control pH values of solutions. Hemin stock solution (0.01 M) was prepared by dissolving required Hemin powder in 0.25% Na_2CO_3 solution. Free Hemin solutions were obtained by diluting the stock solution with PBS.

Apparatus. SEM images were taken by a Nova NanoSEM 230 field-emission microscope. X-ray powder diffraction patterns were measured by a Rigaku Miniflex X-ray diffractometer at 30 kV, 15 mA for Cu Kα (λ = 1.5406 Å) with scan speed of 0.1 s/step and a step size of 0.01°. The specific surface areas of MOF composites were tested by Brunauer–Emmett–Teller (BET) method using nitrogen gas adsorption/desorption at 77 K (BET, Micromeritics ASAP 2020, USA). Microscopic images were obtained by an inverted Eclipse Ti–U microscope (Nikon, Japan) equipped with a color camera (DS-Ri1). UV–vis absorption spectra were measured by a spectrophotometer (Lambda 750, PerkinElmer). CL signals were recorded by an MPI-EII Luminescence Analytical System (Xi'an Remex Analyze Instrument Co. Ltd., China).

Synthesis of Hemin@HKUST-1 Composites. Hemin@HKUST-1 composites were synthesized by a method similar to a previously reported method for preparing Heme doped HKUST-1,[39] except for Heme was displaced by Hemin in the present work. Briefly, 0.5 g of 1,3,5-benzene tricarboxylate and different mass of the Hemin (typically 120 mg) were dissolved in 15 mL ethanol:dimethylformamide (1:1 in volume) mixed solution and further mixed with 7.5 mL of water containing 1.04 g of $Cu(NO_3)_2{\cdot}3H_2O$ in a 50 mL centrifuge tube. The tube was into a water bath (60 °C) for 7 h, then cooled to room temperature. Finally, the composites were collected by centrifugation, washed several times with ethanol until the supernatant was colorless, and vacuum-dried overnight (55 °C). The HKUST-1 composites were synthesized in the same way without the addition of Hemin.

H_2O_2 Detection Using Hemin@HKUST-1 as Solid Mimic Peroxidase. H_2O_2 detection was realized as follows: 10 μL of 1×10^{-3} M luminol (final concentration of 1×10^{-5} M), and 20 μL of 50 mg/mL Hemin@HKUST-1 (final concentration of 1 mg/mL) were added into 960 μL of 10 mM PBS (pH 7.0). As soon as 10 μL of H_2O_2 of different concentrations was injected, the CL signal was measured with the luminescence analyzer.

Glucose Detection Using GOx and Hemin@HKUST-1. Glucose detection was carried out as follows: 100 μL of 1 mg/mL GOx and

DOI: 10.1021/acsami.5b01706
ACS Appl. Mater. Interfaces 2015, 7, 11322–11329

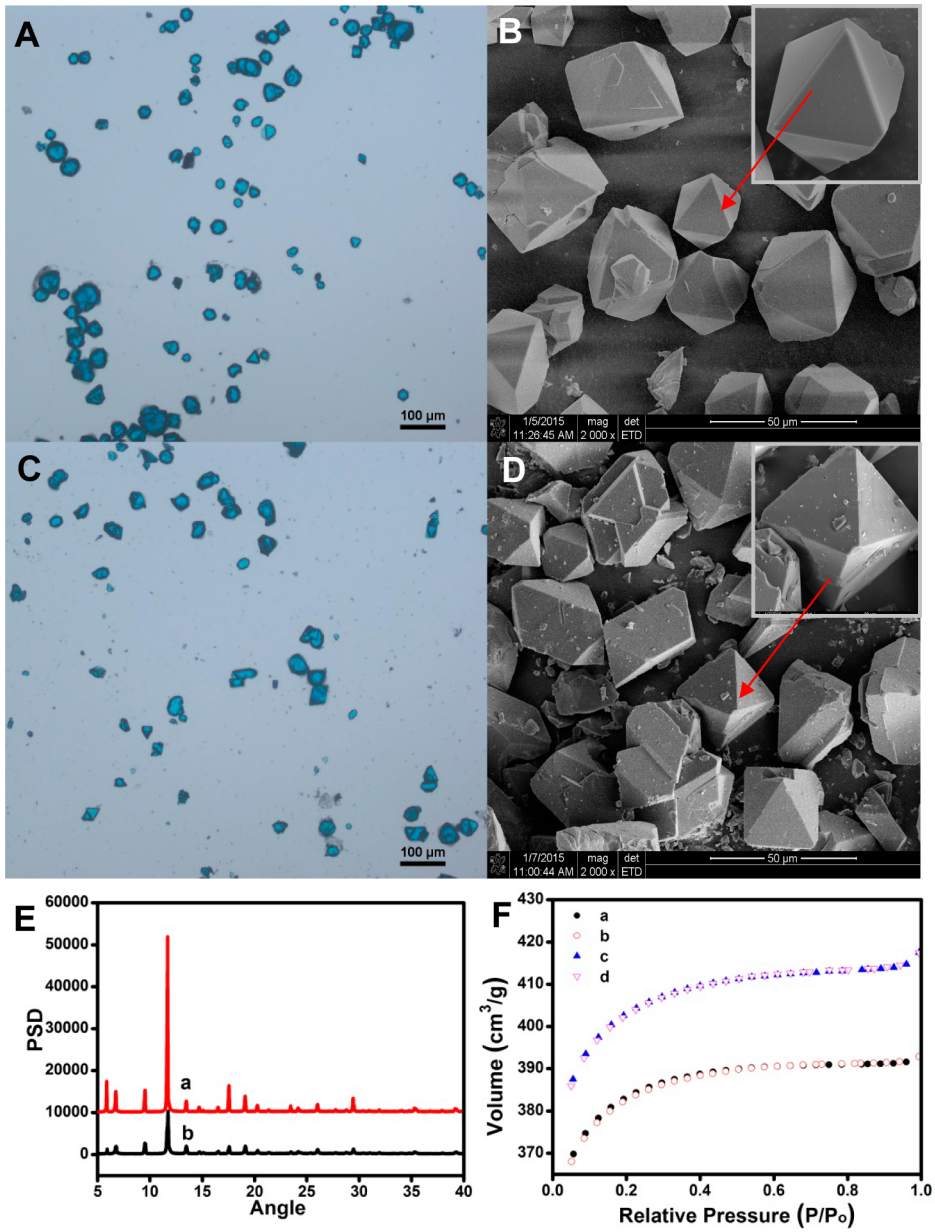

Figure 1. Bright field micrograph image of Hemin@HKUST-1 (A) and HKUST-1 (C). SEM image of Hemin@HKUST-1 (B) and HKUST-1 (D). (E) XRD data for Hemin@HKUST-1 (a) and HKUST-1 (b). (F) N_2 adsorption and desorption isotherms of Hemin@HKUST-1 (a, b) and HKUST-1(c, d).

10 μL of glucose of different concentrations in 860 μL of 10 mM PBS (pH 7.0) were incubated at 37 °C for 30 min, then 20 μL of 50 mg/mL Hemin@HKUST-1 was added into the above glucose reaction solution. Finally, 10 μL of 1×10^{-3} M luminol was injected, and the CL signal was measured with the luminescence analyzer.

RESULTS AND DISCUSSION

Characterization of Hemin@HKUST-1. Under the microscope, the synthesized Hemin@HKUST-1 materials are blue crystals (Figure 1A), which are very similar to the parent MOFs, HKUST-1 (Figure 1C). SEM images clearly show that both Hemin@HKUST-1 (Figure 1B) and bare HKUST-1 (Figure 1D) are essentially the same in morpholoy, i.e. they are define octahedral cystals with average diameter less than 50 μm. Apparently, these images show that the encapsulation of Hemin in HKUST-1 do not change the morpholey of the MOFs. The comparison of the X-ray powder diffraction data of Hemin@HKUST-1 (curve a in Figure 1E) with that of HKUST-1 (cure b in Figure 1E) indicates that the Hemin-doping does not impact the crystalline integrity of HKUST-1. The Brunauer–Emmett–Teller (BET) isotherm experimental results (Figure 1F) suggest that both Hemin@HKUST-1 (curves a and b) and HKUST-1 (curves c and d) exhibit typical type-I isotherm characteristics of microporous materials. The BET surface areas of Hemin@HKUST-1 and HKUST-1 were measured respectively to be 1160.9 and 1222.8 m^2/g, suggesting that the doped Hemin can fill the hole of HKUST-1 somewhat and cause a slight decrease in the BET surface area.

Hemin@HKUST-1 has a small UV–vis absorption peak at 435 nm (curve a in Figure 2), which is assigned to the characteristic UV–vis peak of Hemin (curve b in Figure 2). Around 435 nm, all of $Cu(NO_3)_2$, H_3BTC, and HKUST-1 have no UV–vis absorbances (curves c–e in Figure 2). Therefore, the

DOI: 10.1021/acsami.5b01706
ACS Appl. Mater. Interfaces 2015, 7, 11322–11329

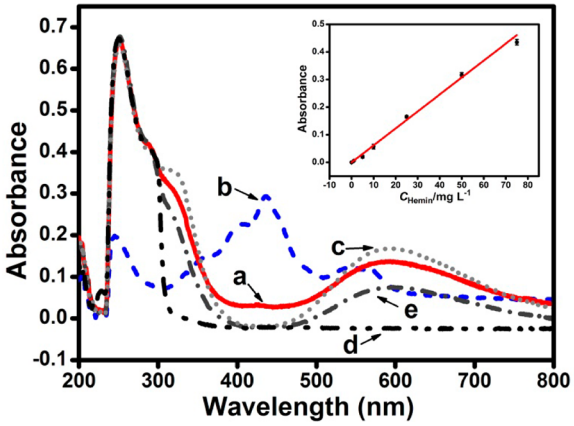

Figure 2. (A) UV−vis absorption spectra of Hemin@HKUST-1 (a), Hemin (b), $Cu(NO_3)_2$ (c), H_3BTC (d), and HKUST-1 (e) solutions dissolved in 250 mM imidazole. (inset) Standard working curve of the absorption intensity at 435 nm versus the known concentration of Hemin. All absorbance was measured in 250 mM imidazole solution.

amount of Hemin in the prepared Hemin@HKUST-1 can be determined by spectrophotometry.[39] In the measurement, a certain weight of Hemin@HKUST-1 was dissolved completely in water containing 0.25 M imidazole that can dissolve HKUST-1 and does not have absorbance around 435 nm, and the concentration of Hemin was measured in the resultant solution based on a spectrophotometric calibration curve (inset of Figure 2). By this analytical method, the content of Hemin incorporated in Hemin@HKUST-1 was determined to be 5.408 mg/g.

Catalytic Activity of Hemin@HKUST-1 for the Luminol−H_2O_2 CL System. In alkaline solution (e.g., 0.1 M NaOH), the catalytic activity of Hemin@HKUST-1 for the CL reaction between luminol and H_2O_2 was investigated. As shown in Figure 3A, no CL was found for luminol−H_2O_2 in the absence of catalyst (see section a in Figure 3A). In contrast, very bright CL emission was observed as soon as Hemin@HKUST-1 was added into luminol−H_2O_2 alkaline solution (see section b in Figure 3A), showing that Hemin@HKUST-1 can strongly catalyze the CL reaction of the luminol−H_2O_2 system. In neutral solution (i.e., pH7.0 PBS), the effect of Hemin@HKUST-1 on the CL intensity was also investigated and shown in Figure 3B. The CL intensity of luminol−H_2O_2 system in the presence of Hemin@HKUST-1 (curve a in Figure 3B) is about 100 times stronger than that of luminol−H_2O_2 system without catalyst (curve b in Figure 3B), whereas there is only a slight increase in CL intensity of the luminol−H_2O_2 system in the prescence of parent MOFs, HKUST-1 (curve c, inset of Figure 3A). Moreover, Figure 1B shows that Hemin@HKUST-1 can quickly catalyze the oxidation of luminol by H_2O_2 and gives rise to a sharp CL signal increase within 5 s, which may be attributed to the low mass transfer resistance in porous structure of MOFs. Additionally, we compared the catalytic activity of Hemin@HKUST-1 with that of free Hemin at the same Hemin concentration (curve d in Figure 3B). The CL intensity of the luminol−H_2O_2 system in the presence of Hemin@HKUST-1 reaches 50% that in the presence of free Hemin. This indicates that the catalytic activity of Hemin is still satisfying after immobilization. Summarily, the above experimental results indicate that Hemin@HKUST-1 exhibits excellent catalytic activities toward the luminol−H_2O_2 CL system both in alkaline and neutral solutions.

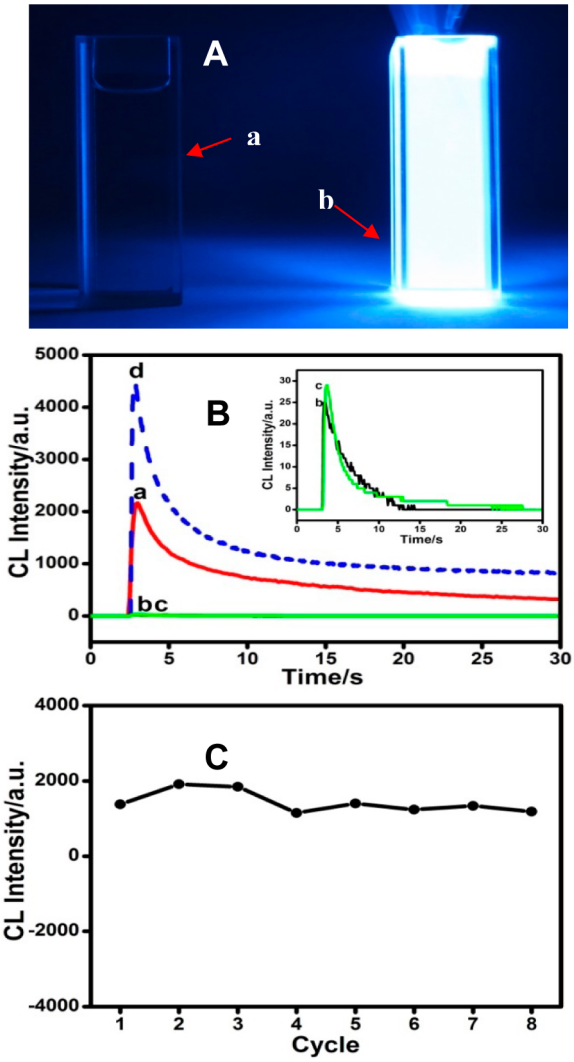

Figure 3. (A) Photographs obtained in the dark for the chemiluminescence reactions of the luminol (0.01M)−H_2O_2 (0.01M) system in NaOH (0.1M) in the absence (a) and presence (b) of Hemin@HKUST-1 (50 mg/mL). (B) CL response curves of the luminol (1.0×10^{-5} M)−H_2O_2 (1.0×10^{-4} M) system in 0.01 M PBS (pH 7.0) in the presence (a) and absence (b) of Hemin@HKUST-1 (1 mg/mL MOFs containing 0.005 mg/mL Hemin), in the presence of bare HKUST-1 (1 mg/mL, curve c), and in the presence of free Hemin (0.005 mg/mL, curve d). (inset) Amplified view of curves b and c. (C) Recycle evaluation for the catalyst of Hemin@HKUST-1. In the first cycle, CL intensity was recorded by adding Hemin@HKUST-1 (1 mg/mL) to the system containing luminol (1.0×10^{-5} M)−H_2O_2 (1.0×10^{-4} M), then Hemin@HKUST-1 was centrifugated from the resultant CL solution and reused for the subsequent CL cycles (2−8).

Recyclability of Hemin@HKUST-1. The recyclability of the catalyst, Hemin@HKUST-1, for the luminol−H_2O_2 CL system was evaluated. A certain weight of Hemin@HKUST-1 was used for catalyzing luminol−H_2O_2 reactions in several CL solutions. After recording the catalytic CL signal from each luminol−H_2O_2 mixed solution, the catalyst (i.e., Hemin@HKUST-1) was separated from the CL reaction solution by centrifugation and added into the next luminol−H_2O_2 mixed solution for catalyzing CL reaction. As shown in Figure 3C, after eight catalysis cycles, the catalyst of Hemin@HKUST-1 still maintained an excellent catalytic activity since the CL

DOI: 10.1021/acsami.5b01706
ACS Appl. Mater. Interfaces 2015, 7, 11322−11329

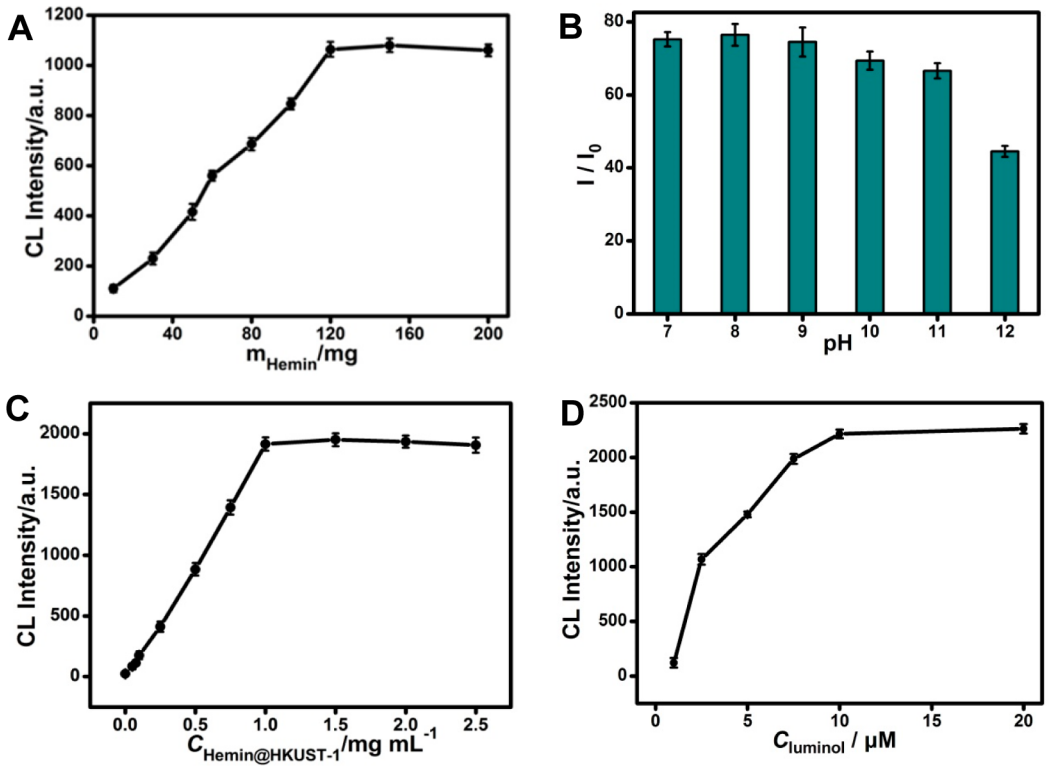

Figure 4. Effects of experimental conditions on the CL intensity of Hemin@HKUST-1-luminol−H_2O_2 sensing system: (A) effect of the mass of Hemin used in the synthesis of Hemin@HKUST-1; (B) effect of pH; (C) effect of the concentration of Hemin@HKUST-1; (D) effect of luminol concentration.

intensity of the Hemin@HKUST-1−luminol−H_2O_2 system does not appear to be much different in the whole process of recycling. The good recyclability of catalyst may be attributed to the fact that the immobilization of Hemin in HKUST-1 enhances Hemin stability and protects the active moiety from dimerization and self-degradation. The experimental results indicate that Hemin@HKUST-1 may be more useful than Hemin since it can be used as a recyclable solid mimic peroxidase.

Optimization of Hemin@HKUST-1-Based CL Sensing Conditions. Since Hemin can catalytic oxidation of luminol by hydrogen peroxide to enhance the CL emission of luminol, the synthesized Hemin@HKUST-1 may be applied for the sensitive detection of H_2O_2 and related enzymatic-linked substrates, such as glucose. Before the establishment of the Hemin@HKUST-1-based CL sensor, several experimental conditions such as the content of Hemin loaded in MOFs, pH value of test solution, the concentration of luminol, and the amount of Hemin@HKUST-1 used on the CL sensing were investigated. First, the content of Hemin in Hemin@HKUST-1 is very important for the catalyst activity of Hemin@HKUST-1. As shown in Figure 4A, the CL intensity is linearly increased with the mass of Hemin as a reactant used in Hemin@HKUST-1 synthesis in the range of 10−120 mg, indicating that the catalytic activity of Hemin@HKUST-1 increases with Hemin content. However, CL intensity tends to be a constant value when more Hemin (>120 mg) is used, suggesting that Hemin in the MOFs reaches its saturated doping concentration, i.e. 5.408 mg/g as mentioned above. Therefore, 120 mg Hemin was chosen for the synthesis of Hemin@HKUST-1. Subsequently, the effect of soltuion pH on the CL intensity of Hemin@HKUST-1−luminol−H_2O_2 system was evaluated and compared with that of free Hemin−luminol−H_2O_2 (Figure S1). As shown in Figure 4B, the CL intensity ratio (I/I_0) of the luminol−H_2O_2 system in the presence or absence of Hemin@HKUST-1 maintains a constant and high value (ca. 78) over pH 7−9, decreases slightly in the range of pH 9−11, and only decrease obviously at pH 12.0. This indicates that Hemin@HKUST-1 exhibits good catalytic activity in a wide pH range (neutral and weakly alkaline solutions). In contrast, the catalytic activity of free Hemin toward luminol−H_2O_2 CL reaction (I/I_0) is significant only at pH 7.0 and has low values over pH 8.0−12.0; especially, there is a sharp decrease in catalytic activity at pH 8.0 (Figure S1). The obvious decrease in free Hemin catalytic activity can be attributed to that dimerization of catalytically active free Hemin into catalytically inactive dimeric species occurs in alkaline solutions.[43] The above comparison between Hemin@HKUST-1 and free Hemin shows that encapsulating Hemin into MOFs may increase the stability of Hemin in aqueous solution and maintain high catalytic activity of Hemin over a wide pH range. It should be noted here that Hemin@HKUST-1 is unstable in the acidic condition, thus pH under 7.0 was not investigated. Considering potential applications of Hemin@HKUST-1−luminol−H_2O_2 in enzymatic-linked detection of biologically interesting molecules such as glucose, pH 7.0 PBS was selected for further experiments. Additionally, the effect of Hemin@HKUST-1 concentration on the CL intensity was studied in the concentration range from 0 to 2.5 mg/mL (Figure 4C). The CL intensity increases with increasing concentrations of Hemin@HKUST-1 up to 1 mg/mL and, thereafter, remains almost constant up to 2.5 mg/mL. Therefore, 1 mg/mL Hemin@HKUST-1 was selected for the present work. Finally, the effect of luminol concentration on the CL intensity of the Hemin@HKUST-1−luminol−H_2O_2

DOI: 10.1021/acsami.5b01706
ACS Appl. Mater. Interfaces 2015, 7, 11322−11329

system was studied. As illustrated in Figure 4D, the CL intensity was found to be enhanced fast with increasing the concentration of luminol in the range of 1−10 μM. But after 10 μM, further increasing the luminol concentration only causes a little rise in CL intensity. Thus, 10 μM luminol was chosen for the CL sensing.

CL Sensing of H_2O_2 and Glucose. For evaluating the applicability of the Hemin@HKUST-1-based CL sensing system for H_2O_2, the linear response range and limit of detection (LOD) were measured under the above-mentioned optimum experimental conditions. As shown in Figure S2, the CL intensity of the Hemin@HKUST-1−luminol−H_2O_2 sensing system increases obviously with the concentration of H_2O_2. There is a good linear correlation between the logarithm of CL intensity (I) and the logarithm of H_2O_2 concentration (C_{H2O2}) in the range from 5.0 to 1000 μM with the following equation:

$$\text{Log } I = 2.203\log C_{H2O2} + 13.26, \qquad (R^2 = 0.9824) \tag{1}$$

The LOD of H_2O_2 was measured to be 2.0 μM when signal-to-noise ratio (S/N) was 3. This is a good result for the detection of H_2O_2 in the neutral condition. When the catalytic reaction of H_2O_2 and luminol by Hemin@HKUST-1 is coupled with the oxidation of glucose catalyzed by GOx, a selective and sensitive detection of glucose can be readily realized. As soon as the enzymatic oxidation of glucose by GOx is finished in the neutral solution for 30 min, the resultant H_2O_2 can be detected by injecting the mixed solution of Hemin@HKUST-1 and luminol. As shown in Figure 5, the logarithm of CL intensity

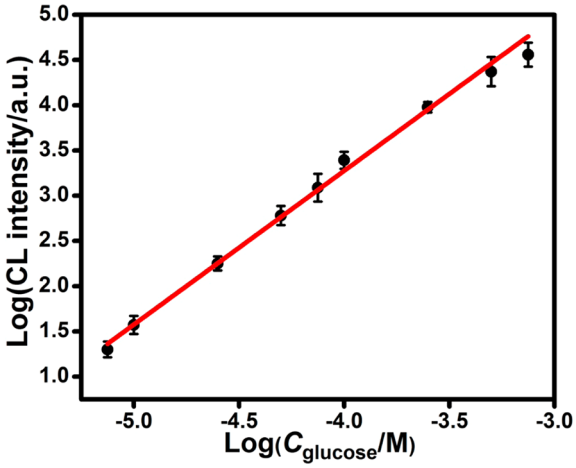

Figure 5. Double logarithmic response of the CL intensity basing on the Hemin@HKUST-1−luminol−H_2O_2 sensors in the detection of different concentration of glucose in 0.01 M PBS (pH 7.0) containing 10 μM luminol and 1 mg/mL Hemin@HKUST-1. The error bars represent the standard deviation in three measurements.

(I) is linearly proportional to the logarithm of glucose concentration ($C_{glucose}$) in the range from 7.5 to 750 μM (eq 2), with a LOD of 7.5 μM (S/N = 3).

$$\text{Log } I = 1.699\log C_{glucose} + 10.07, \qquad (R^2 = 0.9952) \tag{2}$$

Furthermore, to demonstrate the important role of Hemin@HKUST-1 in enhancing the sensing performance, a control experiment, i.e. detecting glucose by luminol CL without the catalysis of Hemin@HKUST-1 (Figure S3) was carried out. The logarithm of CL intensity is linearly proportional to the logarithm of glucose concentration in the range from 75 to 1000 μM, with a LOD of 50 μM (S/N = 3). Compared with CL sensors without Hemin@HKUST-1, the present developed Hemin@HKUST-1-based CL sensors have a higher detection sensitivity, a wider response range and lower LOD, approximately 1 order of magnitude decrease in LOD for target analytes.

Finally, in order to make a comprehensive evaluation on the advantages of the presently developed sensor, we compared the performances between the glucose sensor based on Hemin@HKUST-1 and those based on other solid mimic peroxidases (Table 1).[44−51] It can be known from the comparison that the linear response range (2 order of magnitude) of present glucose sensor is excellent among glucose sensors, and the LOD (7.5 μM) of the presently developed glucose sensor based on Hemin@HKUST-1 can be well matched with most of the recently reported glucose sensors based on various solid mimic peroxidases.

Table 1. Comparison in Performance between the Glucose Sensor Based on Hemin@HKUST-1 and Glucose Sensors Based on Other Solid Mimic Peroxidases

solid mimic peroxidases	detection method	linear range (μM)	LOD (μM)	refs
AuNPs	colorimetry	18−1100	4	44
Hemin−SWCNT	colorimetry	5−50	2	45
CuNCs[a]	colorimetry	100−2000	100	46
TiO_2	electrochemistry	400−3600	5	47
g-C_3N_4[b]	electrochemistry	1000−12000	11	48
Fe_3O_4	fluorescence	1.6−160	1	49
CuO	chemiluminescence	5−60	2.9	50
GO[c]	chemiluminescence	100−2000	82	51
Hemin@HKUST-1	chemiluminescence	7.5−750	7.5	this work

[a]Cu nanoclusters. [b]Graphite-like carbon nitride. [c]Graphene oxide.

CONCLUSIONS

In summary, we reported for the first time encapsulating Hemin into the HKUST-1 materials for chemiluminescence detection of H_2O_2 and glucose in the neutral condition. The synthesized Hemin-functionalized MOFs not only exhibit an excellent catalyst activity inheriting from Hemin but also can be cyclically utilized as solid mimetic peroxidase in the neutral condition. The obtained Hemin@HKUST-1 composites have been used to develop a practical sensor for the detection of H_2O_2 with a wide response range (5 to 1000 μM) and a low LOD of 2 μM, and a sensor for the detection of glucose with a wide response range (7.5 to 750 μM) and a low LOD of 7.5 μM. It is envisioned that the combination of the two different fields of MOFs and chemiluminescence would be widely applied in sensing target analytes in the future.

ASSOCIATED CONTENT

Supporting Information

Figures S1−S3 as mentioned in the text. The Supporting Information is available free of charge on the ACS Publications website at DOI: 10.1021/acsami.5b01706.

AUTHOR INFORMATION

Corresponding Author

*E-mail: y.w.chi@fzu.edu.cn.

DOI: 10.1021/acsami.5b01706
ACS Appl. Mater. Interfaces 2015, 7, 11322−11329

Notes

The authors declare no competing financial interest.

■ ACKNOWLEDGMENTS

This study was financially supported by National Natural Science Foundation of China (21375020, J1103303), Specialized Research Fund for the Doctoral Program of Higher Education of China (20133514110001), and the Program for Changjiang Scholars and Innovative Research Team in University (No. IRT1116).

■ REFERENCES

(1) Gu, Z. Y.; Yang, C. X.; Chang, N.; Yan, X. P. Metal−Organic Frameworks for Analytical Chemistry: From Sample Collection to Chromatographic Separation. *Acc. Chem. Res.* **2012**, *45*, 734−745.

(2) Yaghi, O. M.; O'Keeffe, M.; Ockwig, N. W.; Chae, H. K.; Eddaoudi, M.; Kim, J. Reticular Synthesis and the Design of New Materials. *Nature* **2003**, *423*, 705−714.

(3) Corma, A.; Garciía, H.; Llabreés, I.; Xamena, F. X. Engineering Metal Organic Frameworks for Heterogeneous Catalysis. *Chem. Rev.* **2010**, *110*, 4606−4655.

(4) Lee, J. Y.; Farha, O. K.; Roberts, J.; Scheidt, K. A.; Nguyen, S. T.; Hupp, J. T. Metal−organic Framework Materials as Catalysts. *Chem. Soc. Rev.* **2009**, *38*, 1450−1459.

(5) Li, J. R.; Sculley, J.; Zhou, H. C. Metal−Organic Frameworks for Separations. *Chem. Rev.* **2012**, *112*, 869−932.

(6) Khan1, N. A.; Hasan1, Z.; Jhung, S. H. Adsorptive Removal of Hazardous Materials Using Metal−organic Frameworks (MOFs): A Review. *J. Hazard. Mater.* **2013**, *244−245*, 444−456.

(7) Suh, M. P.; Park, H. J.; Prasad, T. K.; Lim, D. W. Hydrogen Storage in Metal−Organic Frameworks. *Chem. Rev.* **2012**, *112*, 782−835.

(8) Liu, J.; Thallapally, P. K.; McGrail, B. P.; Brown, D. R.; Liu, J. Progress in Adsorption−Based CO_2 Capture by Metal−Organic Frameworks. *Chem. Soc. Rev.* **2012**, *41*, 2308−2322.

(9) Yan, Y.; Yang, S.; Blake, A. J.; Schröder, M. Studies on Metal−Organic Frameworks of Cu(II) with Isophthalate Linkers for Hydrogen Storage. *Acc. Chem. Res.* **2014**, *47*, 296−307.

(10) Langmi, H. W.; Ren, J.; North, B.; Mathe, M.; Bessarabov, D. Hydrogen Storage in Metal−Organic Frameworks: A Review. *Electrochim. Acta* **2014**, *128*, 368−392.

(11) Shvareva, T. Y.; Skanthakumar, S.; Soderholm, L.; Clearfield, A.; Albrecht-Schmitt, T. E. Cs^+ −Selective Ion Exchange and Magnetic Ordering in a Three−Dimensional Framework Uranyl Vanadium(IV) Phosphate. *Chem. Mater.* **2007**, *19*, 132−134.

(12) Nouar, F.; Eckert, J.; Eubank, J. F.; Forster, P.; Eddaoudi, M. Zeolite-like Metal−Organic Frameworks (ZMOFs) as Hydrogen Storage Platform: Lithium and Magnesium Ion−Exchange and H_2 − (rho−ZMOF) Interaction Studies. *J. Am. Chem. Soc.* **2009**, *131*, 2864−2870.

(13) Kreno, L. E.; Leong, K.; Farha, O. K.; Allendorf, M.; Duyne, R. P. V.; Hupp, J. T. Metal−Organic Framework Materials as Chemical Sensors. *Chem. Rev.* **2012**, *112*, 1105−1125.

(14) Della Rocca, J.; Liu, D.; Lin, W. Nanoscale Metal-Organic Frameworks for Biomedical Imaging and Drug Delivery. *Acc. Chem. Res.* **2011**, *44*, 957−968.

(15) Huxford, R. C.; Della Rocca, J.; Lin, W. Metal−Organic Frameworks as Potential Drug Carriers. *Curr. Opin. Chem. Biol.* **2010**, *14*, 262−268.

(16) Mckinlay, A. C.; Morris, R. E.; Horcajada, P.; Férey, G.; Gref, R.; Couvreur, P.; Serre, C. BioMOFs: Metal−Organic Frameworks for Biological and Medical Applications. *Angew. Chem., Int. Ed.* **2010**, *49*, 6260−6266.

(17) Heitbaum, M.; Glorius, F.; Escher, I. Asymmetric Heterogeneous Catalysis. *Angew. Chem., Int. Ed.* **2006**, *45*, 4732−4762.

(18) Yoon, M.; Srirambalaj, R.; Kim, K. Homochiral Metal−Organic Frameworks for Asymmetric Heterogeneous Catalysis. *Chem. Rev.* **2012**, *112*, 1196−1231.

(19) Dhakshinamoorthy, A.; Garcia, H. Catalysis by Metal Nanoparticles Embedded on Metal−Organic Frameworks. *Chem. Soc. Rev.* **2012**, *41*, 5262−5284.

(20) Horike, S.; Dinca, M.; Tamaki, K.; Long, J. R. Size-Selective Lewis Acid Catalysis in a Microporous Metal−Organic Framework with Exposed Mn^{2+} Coordination Sites. *J. Am. Chem. Soc.* **2008**, *130*, 5854−5855.

(21) Tanabe, K. K.; Cohen, S. M. Engineering a Metal−Organic Framework Catalyst by Using Postsynthetic Modification. *Angew. Chem., Int. Ed.* **2009**, *121*, 7560−7563.

(22) Ma, L.; Lin, W. Designing Metal−Organic Frameworks for Catalytic Applications. *Top. Curr. Chem.* **2010**, *293*, 175−205.

(23) Lillerud, K. P.; Olsbye, U.; Tilset, M. Designing Heterogeneous Catalysts by Incorporating Enzyme−Like Functionalities into MOFs. *Top. Catal.* **2010**, *53*, 859−868.

(24) Juan-Alcañiz, J.; Gascon, J.; Kapteijn, F. Metal−Organic Frameworks as Scaffolds for the Encapsulation of Active Species: State of the Art and Future Perspectives. *J. Mater. Chem.* **2012**, *22*, 10102−10118.

(25) Lu, G.; Li, S.; Guo, Z.; Farha, O. K.; Hauser, B. G.; Qi, X.; Wang, Y.; Wang, X.; Han, S.; Liu, X.; DuChene, J. S.; Zhang, H.; Zhang, Q.; Chen, X.; Ma, J.; Loo, S. C. J.; Wei, W. D.; Yang, Y.; Hupp, J. T.; Huo, F. Nature Imparting Functionality to a Metal−Organic Framework Material by Controlled Nanoparticle Encapsulation. *Nat. Chem.* **2012**, *4*, 310−316.

(26) Gu, X.; Lu, Z. H.; Jiang, H. L.; Akita, T.; Xu, Q. Synergistic Catalysis of Metal−Organic Framework-Immobilized Au−Pd Nanoparticles in Dehydrogenation of Formic Acid for Chemical Hydrogen Storage. *J. Am. Chem. Soc.* **2011**, *133*, 11822−11825.

(27) Sadakiyo, M.; Kon-no, M.; Sato, K.; Nagaoka, K.; Kasai, H.; Kato, K.; Yamauchi, M. Synthesis and Catalytic Application of PVP−Coated Ru Nanoparticles Embedded in a Porous Metal−Organic Framework. *Dalton. Trans.* **2014**, *43*, 11295−11298.

(28) Zhao, M.; Ou, S.; Wu, C. D. Porous Metal−Organic Frameworks for Heterogeneous Biomimetic Catalysis. *Acc. Chem. Res.* **2014**, *47*, 1199−1207.

(29) Gu, Z. Y.; Park, J.; Raiff, A.; Wei, Z.; Zhou, H. C. Metal−Organic Frameworks as Biomimetic Catalysts. *Chem. Catal. Chem.* **2014**, *6*, 67−75.

(30) Alkordi, M. H.; Liu, Y.; Larsen, R. W.; Eubank, J. F.; Eddaoudi, M. Zeolite−like Metal−Organic Frameworks as Platforms for Applications: On Metalloporphyrin−Based Catalysts. *J. Am. Chem. Soc.* **2008**, *130*, 12639−12641.

(31) Zalomaeva, O. V.; Kovalenko, K. A.; Chesalov, Y. A.; Mel'gunov, M. S.; Zaikovskii, V. I.; Kaichev, V. V.; Sorokin, A. B.; Kholdeeva, O. A.; Fedin, V. P. Iron Tetrasulfophthalocyanine Immobilized on Metal Organic Framework MIL−101: Synthesis, Characterization and Catalytic Properties. *Dalton. Trans.* **2011**, *40*, 1441−1444.

(32) Feng, D.; Gu, Z. Y.; Li, J. R.; Jiang, H. L.; Wei, Z.; Zhou, H. C. Zirconium−Metalloporphyrin PCN−222: Mesoporous Metal−Organic Frameworks with Ultrahigh Stability as Biomimetic Catalysts. *Angew. Chem., Int. Ed.* **2012**, *51*, 10307−10310.

(33) Fateeva, A.; Chater, P. A.; Ireland, C. P.; Tahir, A. A.; Khimyak, Y. Z.; Wiper, P. V.; Darwent, J. R.; Rosseinsky, M. J. A Water−Stable Porphyrin−Based Metal−Organic Framework Active for Visible−Light Photocatalysis. *Angew. Chem., Int. Ed.* **2012**, *51*, 7440−7444.

(34) Zhang, Z.; Zhang, L.; Wojtas, L.; Nugent, P.; Eddaoudi, M.; Zaworotko, M. J. Templated Synthesis, Postsynthetic Metal Exchange, and Properties of a Porphyrin−Encapsulating Metal−Organic Material. *J. Am. Chem. Soc.* **2012**, *134*, 928−933.

(35) Zhang, Z.; Wojtas, L.; Eddaoudi, M.; Zaworotko, M. J. Stepwise Transformation of the Molecular Building Blocks in a Porphyrin−Encapsulating Metal−Organic Material. *J. Am. Chem. Soc.* **2013**, *135*, 5982−5985.

(36) Suslick, K. S.; Rakow, N. A.; Kosal, M. E.; Chou, J. H. The Materials Chemistry of Porphyrins and Metalloporphyrins. *J. Porphyr. Phthalocya.* **2000**, *4*, 407−413.

DOI: 10.1021/acsami.5b01706
ACS Appl. Mater. Interfaces 2015, 7, 11322−11329

(37) Ai, L.; Li, L.; Zhang, C.; Fu, J.; Jiang, J. MIL-53(Fe): A Metal−Organic Framework with Intrinsic Peroxidase-like Catalytic Activity for Colorimetric Biosensing. *Chem.−Eur. J.* **2013**, *19*, 15105−15108.
(38) Zhang, J. W.; Zhang, H. T.; Du, Z. Y.; Wang, X.; Yu, S. H.; Jiang, H. L. Water-Stable Metal−Organic Frameworks with Intrinsic Peroxidase-Like Catalytic Activity as A Colorimetric Biosensing Platform. *Chem. Commun.* **2014**, *50*, 1092−1094.
(39) Larsen, R. W.; Wojtas, L.; Perman, J.; Musselman, R. L.; Zaworotko, M. J.; Vetromile, C. M. Mimicking Heme Enzymesin the Solid State: Metal−Organic Materials with Selectively Encapsulated Heme. *J. Am. Chem. Soc.* **2011**, *133*, 10356−10359.
(40) Bastos, E. L.; Romoff, P.; Eckert, C. R.; Baader, W. J. Evaluation of Antiradical Capacity by H_2O_2 −Hemin−Induced Luminol Chemiluminescence. *J. Agric. Food. Chem.* **2003**, *51*, 7481−7488.
(41) Pavlov, V.; Xiao, Y.; Gill, R.; Dishon, A.; Kotler, M.; Willner, I. Amplified Chemiluminescence Surface Detection of DNA and Telomerase Activity Using Catalytic Nucleic Acid Labels. *Anal. Chem.* **2004**, *76*, 2152−2156.
(42) Shlyahovsky, B.; Li, D.; Katz, E.; Willner, I. Proteins modified with DNAzymes or aptamers act as biosensors or biosensor labels. *Biosens. Bioelectron.* **2007**, *22*, 2570−2576.
(43) Satterlee, J. D.; Shelnutt, J. A. Characterization of pH dependent axial ligation changes of monomer and dimer forms of iron(III) uroporphyrin I in aqueous solution. *Inorg. Chim. Acta* **1985**, *106*, 165−170.
(44) Jv, Y.; Li, B.; Cao, R. Positively-Charged Gold Nanoparticles as Peroxidiase Mimic and Their Application in Hydrogen Peroxide and Glucose Detection. *Chem. Commun.* **2010**, *46*, 8017−8019.
(45) Zhang, Y.; Xu, C.; Li, B. Self-assembly of Hemin on Carbon Nanotube as Highly Active Peroxidase Mimetic and Its Application for Biosensing. *RSC Adv.* **2013**, *3*, 6044−6050.
(46) Hu, L.; Yuan, Y.; Zhang, L.; Zhao, J.; Majeed, S.; Xu, G. Copper Nanoclusters As Peroxidase Mimetics and Their Applications to H_2O_2 and Glucose Detection. *Anal. Chim. Acta* **2013**, *762*, 83−86.
(47) Zhang, L.; Han, L.; Hu, P.; Wang, L.; Dong, S. TiO_2 Nanotube Arrays: Intrinsic Peroxidase Mimetics. *Chem. Commun.* **2013**, *49*, 10480−10482.
(48) Tian, J.; Liu, Q.; Ge, C.; Xing, Z.; Asiri, A. M.; Al-Youbi, A. O.; Sun, X. Ultrathin Graphitic Carbon Nitride Nanosheets: A Low-Cost, Green, and Highly Efficient Electrocatalyst Glucose Biosensing Application. *Nanoscale.* **2013**, *5*, 8921−8924.
(49) Gao, Y.; Wang, G.; Huang, H.; Hu, J.; Shah, S. M.; Su, X. Fluorometric Method for the Determination of Hydrogen Peroxide and Glucose with Fe_3O_4 as Catalyst. *Talanta.* **2011**, *85*, 1075−1080.
(50) Chen, W.; Hong, L.; Liu, A. L.; Liu, J. Q.; Lin, X. H.; Xia, X. H. Enhanced Chemiluminescence of the Luminol-Hydrogen Peroxide System by Colloidal Cupric Oxide Nanoparticles as Peroxidase Mimic. *Talanta.* **2012**, *99*, 643−648.
(51) Hao, M.; Liu, N.; Ma, Z. A New Luminol Chemiluminescence Sensor for Glucose Based on pH-Dependent Graphene Oxide. *Analyst.* **2013**, *138*, 4393−4397.

DOI: 10.1021/acsami.5b01706
ACS Appl. Mater. Interfaces 2015, 7, 11322−11329